Manuscript Refereed by Prof Xiaoyan Song (Beijing University of Technology, China)

TiSiCN Nanocomposite Hard Coatings by CVD

Mandy Höhn (Fraunhofer IKTS, Winterbergstraße 28, D-01277 Dresden, Germany) mandy.hoehn@ikts.fraunhofer.de; Ingolf Endler (Fraunhofer IKTS, Winterbergstraße 28, D-01277 Dresden, Germany) ingolf.endler@ikts.fraunhofer.de; Björn Matthey (Fraunhofer IKTS, Winterbergstraße 28, D-01277 Dresden, Germany) bjoern.matthey@ikts.fraunhofer.de

Abstract
TiN and TiC_xN_y are commercial CVD coatings widely used for cutting tool applications. A promising route for improving hardness and oxidation resistance is the addition of silicon. Therefore investigations were performed using a moderate temperature CVD process with a gas mixture containing $TiCl_4$, $SiCl_4$ and CH_3CN. This work is focused on the investigation of structure, composition and properties of the TiSiCN coatings deposited on hardmetal inserts. The precursor ratio $SiCl_4$ to $TiCl_4$ was varied. The structure was analyzed by SEM, TEM and XRD. A maximum hardness about 40 GPa was observed at a silicon content around 12 at.%. In this silicon concentration range a TiC_xN_y grain size below 20 nm was determined. The investigation of the oxidation behavior shows an increase of the oxidation resistance with the silicon content. The TiSiCN CVD coatings show a high performance in different cutting tests.

1. Introduction

TiN and TiC_xN_y are commercial Chemical Vapor Deposition (CVD) based coatings widely used for cutting tool applications [1]. It is well known that TiN as well as TiC_xN_y coatings oxidize in dry oxygen or air at temperatures as low as 500°C [2, 3]. However cutting applications like high speed milling will cause temperatures between 800 and 1200°C [4]. A promising route for improving such layers in terms of hardness and oxidation resistance is the addition of silicon. If silicon is incorporated as silicon nitride, carbonitride or carbide an improved oxidation resistance can be expected. Furthermore a nanocomposite structure consisting of non-miscible nanocrystalline and amorphous phases allows a high hardness [5].
Since 1992 TiSiN nanocomposite layers have been developed using plasma-enhanced Chemical Vapor Deposition (PECVD) and Physical Vapor Deposition (PVD) methods [5-10]. The further development also led to TiSiCN nanocomposites prepared by different PVD as well as PECVD processes [11-14]. These coatings are characterized by an increased hardness and oxidation resistance as well as a decreased friction coefficient for sliding against steel [15-17]. From investigations with TiSiN layers it is known that the oxidation behavior is improved by formation of $TiSi_2$-a-Si_3N_4-TiN mixtures [18] or coatings with crystalline TiN and amorphous SiN_x phases [19]. Generally coatings prepared with PVD and PECVD show similar hardness and properties.
TiSiN and TiSiCN nanocomposites are materials consisting of nanocrystalline TiN or TiC_xN_y with crystal size below 100 nm and a surrounding amorphous phase. Such nanocomposites offer excellent mechanical properties. On the one hand the Hall-Petch relationship is valid where a decrease of the crystallite size leads to an increasing hardness of the composite. On the other hand such nanocomposites show a high resistance against crack formation [16]. Usually such nanocomposites are deposited at low temperatures and there are only a few studies using thermal CVD. In early works Si_3N_4-TiN composite coatings were prepared between 1050°C and 1450°C [20, 21]. At 1050°C a composite was obtained consisting of nanocrystalline TiN with a content of 31.1 wt.% in an amorphous Si_3N_4 matrix. The nanocrystalline TiN was finely dispersed in a large amount of the amorphous matrix. But this is not comparable with the above mentioned nanocomposites having only a very thin amorphous matrix. Atmospheric pressure CVD (APCVD) of TiSiN and TiSiCN at different temperature ranges was investigated by Kuo et al. [22-24]. Deposition of TiSiN coatings with a gas mixture of $TiCl_4$, $SiCl_4$, NH_3 and Ar was carried out in the temperature range between 650°C and 800°C [22]. A composite TiN/amorphous Si_3N_4 was formed achieving a maximum hardness of 21.5 GPa at 800°C. However a detailed structure analysis was not performed. In a further publication Kuo et al. [23] examined CVD of quaternary Ti-Si-C-N coatings in the range of 700°C – 1100°C with $TiCl_4$, $SiCl_4$, C_2H_2, H_2, N_2 and Ar as feed gases. The resulting deposits are a (Ti,Si)(C,N) solid solution with TiC structure. The same group applied also another CVD process in the range of 650° - 800°C with $TiCl_4$, $SiCl_4$, C_2H_2, NH_3 and Ar [24]. TiSiCN coatings with low carbon content and a nanoscale microstructure were obtained. The low carbon content is caused by the higher reactivity of NH_3 compared to C_2H_2. In these coatings TiN and $TiN_{0.3}$ were analyzed as crystalline phases but not TiC_xN_{1-x}. Because of the low carbon content Si_3N_4 is assumed as amorphous phase.

In an earlier publication we reported about improvements of hardness and oxidation stability of TiSiN and TiSiCN layers prepared with a low pressure CVD (LPCVD) process [25]. This work is focussed to more detailed investigations of structure, composition, properties and wear behavior of the TiSiCN coatings deposited on hardmetal inserts by LPCVD.

2. Experimental

2.1 CVD process

The LPCVD coating processes was carried out in a horizontal hot wall reactor made of Inconel, which has an inner diameter of 79 mm and a length of 1.2 m. The substrate temperature is controlled by a K-Type thermocouple. All CVD processes were carried out at moderate temperatures between 800°C and 900°C and at pressures of 6 kPa. The flow rates of all gases are controlled by mass flow controllers. Liquid precursors were evaporated by bubbler systems with H_2 carrier gas held at different temperatures: $TiCl_4$ at 60°C, $SiCl_4$ at 20°C and CH_3CN at 20°C. The applied gases have a purity of 99.999% for Ar and N_2, and 99.9% for H_2 which is further cleaned by an Oxisorb cartridge. The purity of $TiCl_4$, $SiCl_4$ and CH_3CN is 98%, 99% and 99.9%, respectively.
The TiSiCN coatings were prepared with fixed $SiCl_4$ and CH_3CN flow rates of 20.4 sccm and 7.9 sccm and at a total gas flow of 3.5 slm. The substrate temperature was varied in the range between 800°C and 900°C and the $TiCl_4$ flow rate was adjusted between 2.5 sccm and 13.9 sccm.
All TiSiCN coatings except coatings for cutting tests were deposited on cemented carbide substrates with 6% Co (WC grain size 1 µm, geometry SNUN120408) having a commercial CVD pre-coating system of TiN/TiC_xN_y/TiN (Kennametal). The pre-coating system prevents unwanted reactions between silicon and cobalt binder of hard metal and ensures a good layer adhesion. In all cases the cemented carbide substrates were cleaned in ethanol in an ultrasonic bath before layer deposition. For all investigations regarding to composition and microstructure a typical TiSiCN film thickness about 5 µm was applied.

2.2 Analysis methods

The coating thickness was measured on calotte sections, and the layer quality was evaluated by optical light microscopy. The preparation of the calotte section was always carried out on a sample having the identical position in the reactor in order to exclude differences due to flow effects. The microstructure and the composition of the coatings were characterized by means of metallography, by field emission scanning electron microscopy (FESEM - LEO 982), transmission electron microscopy (TEM JEOL 2100F), X-ray diffraction with Bragg-Brentano configuration (XRD7 - Seifert FPM) and glancing incidence technique (XRD - Seifert-FPM 3003TT), energy-dispersive and wavelength-dispersive X-ray spectroscopy (EDX, WDX). Types and manufacturers of the applied EDX and WDX equipment are INCA Energy 350 of Oxford Instruments and WDX-3PC of Microspec Corporation, respectively. X-ray diffraction analyses were performed with Cu-Kα radiation. Glancing incidence XRD is carried out with a flat angle of 1°. The microhardness was determined by the Vickers method (Anton Paar MHT 10) using a load of 0.1 N. The average over five measurements was formed. The hardness was measured on a calotte section in the top area of the investigated layer.
The oxidation behavior was investigated by annealing coated cemented carbide substrates at different temperatures for 1 h in air followed by characterization with XRD. For every oxidation temperature a new sample was used. The layers were annealed at 700°C, 800°C, 900°C and 1000°C and the analysis was conducted with glancing incidence XRD at a flat angle 3°.
Wear test were carried out by dry milling and dry boring of cast iron GGG40. The details of the cutting test conditions are listed in Section 3.4.

3. Results and discussion

3.1 Composition and microstructure

Because of the experience with undesirable interface reaction with cobalt in earlier work [25] the deposition of TiSiCN was always performed on an interlayer system TiN/TiC_xN_y/TiN with a thickness of 5 µm. The TiSiCN coatings used for composition and structure analyses have also a thickness about 5 µm. XRD pattern at different substrate temperatures exhibit only reflexes of TiC_xN_y without any other crystalline phases. This means that the only crystalline phase in the TiSiCN coating is TiC_xN_y. There was no silicide formation observable at all experiments using the interlayer system TiN/TiC_xN_y/TiN. For increasing $SiCl_4/TiCl_4$ ratio and therefore with rising silicon content the texture of the TiC_xN_y changes from <220> to <200>. The texture changes if the silicon content exceeds 4 at.%.
Pure MT-TiCN films deposited with acetonitrile show either a <220> texture also described by Czettl et al. [26] or a <211> texture obtained by Larsson and Ruppi [27]. Different gas phase compositions in the MT-TiCN processes could be a reason for developing both textures for example the use of different nitrogen contents. In TiSiCN composite coatings the texture is influenced by silicon carbonitride which surrounds the grain boundaries of the TiC_xN_y crystals. Obviously the grain growth in

the <220> direction is suppressed if TiC_xN_y crystals are covered by the amorphous SiC_xN_y boundary phase. Developing of a <200> texture due to SiN_x or SiC_xN_y addition was also observed in TiSiN and TiSiCN coatings prepared by PVD [28, 29].
WDX analyses listed in Table 1 show generally an increase of the silicon content with rising $SiCl_4/TiCl_4$ ratio and temperature. But there are also some irregularities. At the highest $SiCl_4/TiCl_4$ ratio at 850°C the silicon content drops down comparable to prior examinations in the TiSiN system [26]. If the $SiCl_4/TiCl_4$ ratio is adjusted from 1.5 to 8.2 the $CH_3CN/(SiCl_4 + TiCl_4)$ ratio changes slightly between 0.23 and 0.35 however the $CH_3CN/TiCl_4$ ratio increases strongly from 0.6 to 3.2. An increasing $CH_3CN/TiCl_4$ ratio leads to a rising TiC_xN_y deposition rate which damps the silicon incorporation.

Table 1: Composition of TiSiCN layers in dependence on substrate temperature T_S and $SiCl_4/TiCl_4$ ratio

T_S °C	$SiCl_4/TiCl_4$ ratio	Si content at.%	Ti content at.%	C content at.%	N content at.%	O content at.%	Cl content at.%
800	4.9	11.7	36.9	27.4	20.8	2.8	0.39
850	1.5	0.1	42.5	29.5	25.0	2.9	0.01
850	4.9	4.8	41.2	27.6	24.0	2.4	0.01
850	6.2	11.1	34.7	27.6	23.6	2.7	0.26
850	8.2	4.1	42.3	27.0	23.9	2.7	0.04
900	1.5	0.2	42.1	31.3	23.2	3.2	0.01
900	2.5	2.2	43.4	29.2	22.6	2.5	0.01
900	4.9	5.3	41.3	27.4	23.1	2.9	0.02
900	6.2	22.2	23.9	29.9	21.4	2.2	0.43

Another observation originating from different effects of $SiCl_4$ is mentioned by Kuo et al. [24] for APCVD of TiSiCN coatings below 800°C. $SiCl_4$ can act as a growth accelerator at low $SiCl_4$ flow rate while it acts as a growth inhibitor at high $SiCl_4$ flow rate. In our process conditions the $SiCl_4$ flow is constant but the fraction of $SiCl_4$ increases and therefore such effects can also play a role at the lower temperatures. At 900°C the reactivity of $SiCl_4$ with CH_3CN is higher and a continuous silicon incorporation results.
Crystallite size determination by Rietveld analysis of the XRD pattern gives values of 26 nm and 19 nm for coatings with silicon contents of 4.14 at.% and 11.74 at.% , respectively. Earlier investigations with XPS showed that the amorphous phase is a carbon-rich SiC_xN_y [25]. In Fig. 1a) a high resolution SEM image of a cross section of the complete layer system is shown. Further investigations by TEM analysis show a columnar structure of TiC_xN_y nanocrystals embedded in the SiC_xN_y matrix.

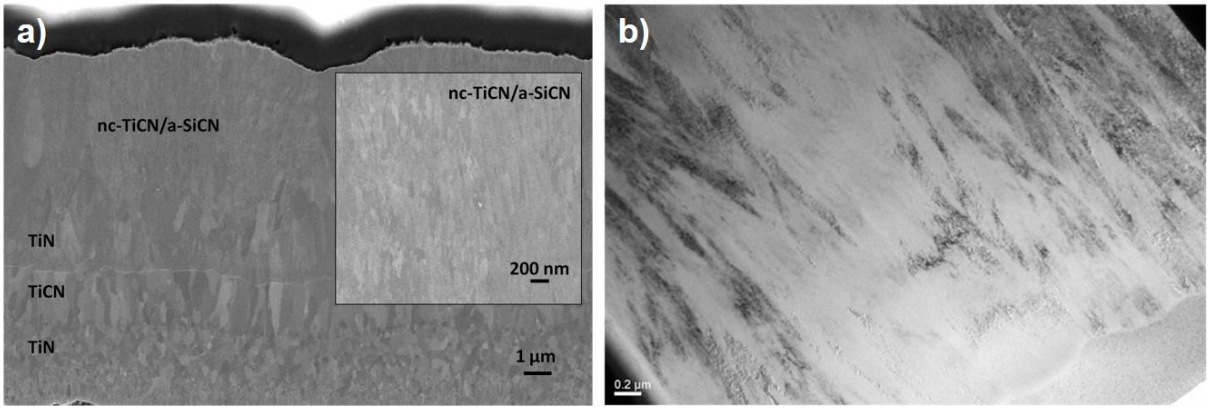

Fig. 1: a) SEM image of a cross section of a complete layer system consisting of a $TiN/TiC_xN_y/TiN$ precoating a the nc-TiC_xN_y/a-SiC_xN_y top coating; b) TEM image of the nc-TiC_xN_y/a-SiC_xN_y coating

3.2 Hardness

Correlations between the hardness of the TiSiCN coatings and the crystallite size of TiC_xN_y as well as the silicon content are presented in Fig. 2. A clear dependence of the hardness from the silicon content can be observed. The highest hardness of 4100 HV[0.01] is achieved at a silicon content of 11.74 at.% and a TiC_xN_y crystallite size of 19 nm. In the case of the TiSiCN nanocomposite there is an interaction of two contributions. On the one hand the hardness increases due to a reduction of the TiC_xN_y crystallite size according to the Hall-Petch relation. On the other hand the amorphous carbon-rich SiC_xN_y is also a phase with a high hardness and contributes to the composite hardness. A further increase of the silicon content to 22 at.% lead to a further refinement of the crystal size to 12 nm but

also to a remarkable decrease of the hardness. The thickness of the amorphous interface layer increases and the area of the optimal nanocomposite structure is left. The lower hardness of the amorphous matrix becomes predominant.

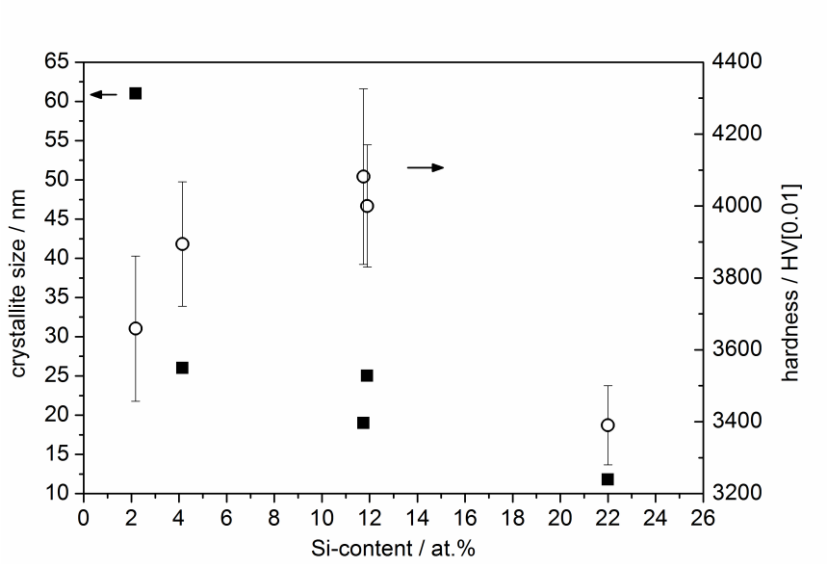

Fig. 2: Crystallite size and hardness of TiSiCN coatings in dependence on the Si-content

3.3 Oxidation behavior

TiSiCN nanocomposite coatings prepared by CVD should also exhibit an improved oxidation resistance. TiSiCN coatings with different silicon contents of 2.8 at.% and 9.6 at.% and a phase composition nc-TiC_xN_y/a-SiC_xN_y were chosen for oxidation test. The TiSiCN coated cemented carbide substrates were annealed at 700°C, 800°C, 900°C and 1000°C in air for 1 hour followed by characterization with XRD with glancing incidence at a flat angle of 3°. For every oxidation temperature a new sample was used. Fig. 3 shows the XRD diffractograms of both the as-deposited and the oxidized samples with lower and higher silicon contents. At 700°C the oxidation starts forming anatase for both layers. The intensities for anatase are much lower in the diffractogramm for the sample with the higher silicon content. The TiC_xN_y structure survive even up to an oxidation temperature of 900°C as can be seen at the band in the 2Θ range 42° - 44°. This is a surprising high oxidation stability suggesting to a favorable structure of the TiSiCN nanocomposite with TiC_xN_y nanocrystals surrounded by a protecting SiC_xN_y shell. At 900°C formation of rutile is favored for the sample with the lower silicon content. For the sample with the higher silicon content a mixture of anatase and rutile is formed. At an oxidation temperature of 1000°C bands only of rutile are detected. Obviously the carbon-rich nature of the coatings favors the anatase formation at lower oxidation temperatures as described for carbon-rich TiC_xN_y [30]. At higher oxidation temperatures the thermodynamic stable rutile is formed.

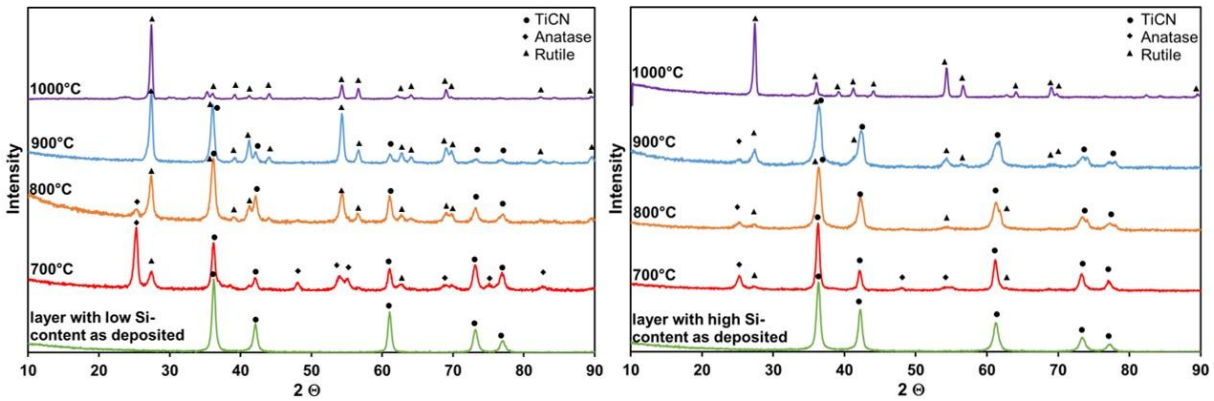

Fig. 3: XRD diffractograms of TiSiCN coatings with a low Si-content of 2.8 at.% (left) and a higher Si-content of 9.6 at.% before and after annealing in air for 1 h at 700°C, 800°C, 900°C and 1000°C

3.4 Cutting tests

For determination of the wear resistance of the new nanocomposite consisting of nc-TiC_xN_y and carbon-rich a-SiC_xN_y cutting tests with cast iron GGG40 were performed. As substrates cemented carbides with 6% Co for milling (fine-grained WC, geometry CTHQ) and with 9% Co for boring (fine-grained WC, geometry WTHQ) with a pre-coating system of TiN/TiC_xN_y/TiN were used. For dry milling of GGG40 following cutting conditions were chosen: v_c= 200 m/min, f_z = 0.2 mm/U and a_p = 2 mm. As second wear test dry boring of GGG40 with the cutting conditions v_c= 200 m/min, f_z = 0.2 mm/U and a_p = 1 mm were performed. These both wear tests reveal an excellent life time of the new CVD TiSiCN nanocomoposite coatings in machining of cast iron. Fig. 4 and Fig. 5 illustrate the high performance of TiSiCN coatings in dry milling and dryboring of GGG40. The tool life is increased by more than 30 percent compared to a state-of-the-art PVD TiAlN coating. Furthermore the cutting edge of the TiSiCN coated insert at the end of the tool life in Fig. 4 shows a more uniform flank wear for milling GGG40. CVD TiSiCN nanocomposite coatings are a promising candidate for the next generation of wear resistant tool coatings due to their high hardness, oxidation resistance as well as excellent performance in machining cast iron.

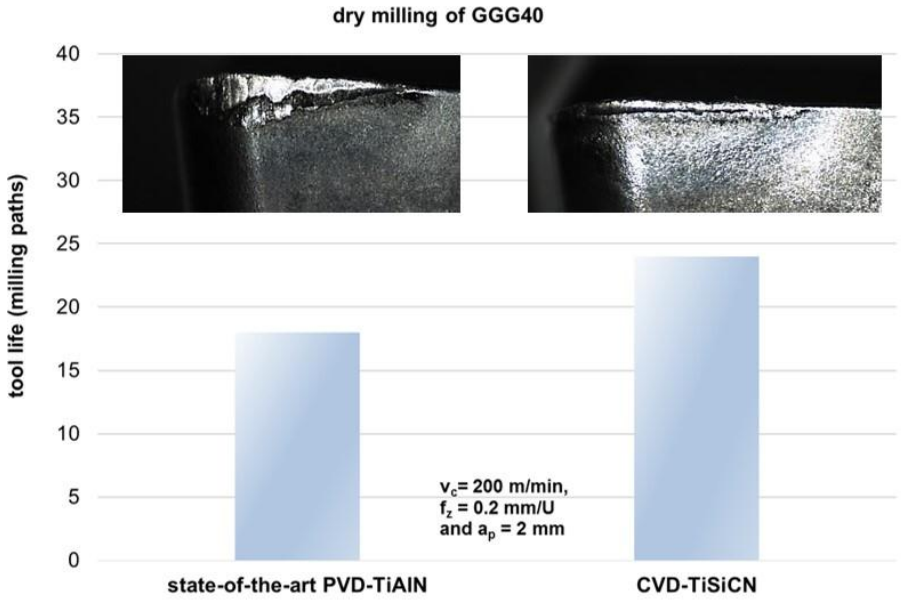

Fig. 4: Cutting test dry milling of GGG40 with the new nanocomposite TiSiCN coating in comparison with an state-of-the-art PVD TiAlN layer

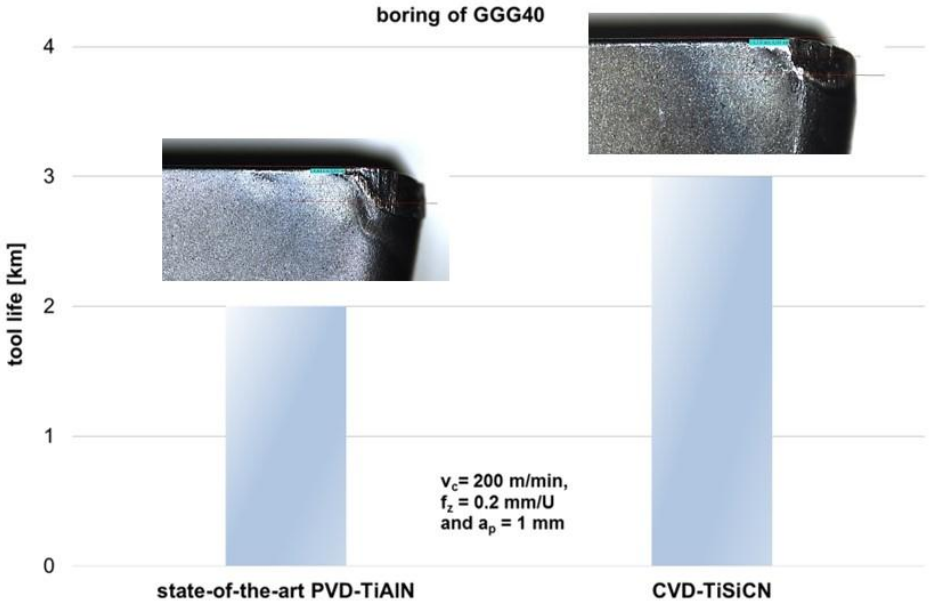

Fig. 5: Cutting test dry boring of GGG40 with the new nanocomposite TiSiCN coating in comparison with an state-of-the-art PVD TiAlN layer

4 Summary and conclusions

At moderate temperatures between 800°C and 900°C TiSiCN nanocomposite layers could be prepared successfully by a LPCVD process using a gas mixture of $TiCl_4$, $SiCl_4$, CH_3CN, H_2, and Ar . Microstructure, composition, hardness, oxidation and wear behavior were investigated. The TiSiCN coatings contain nanocrystalline TiC_xN_y in a columnar structure and amorphous carbon-rich SiC_xN_y. The crystallite size of TiC_xN_y decreases with rising silicon content. At a silicon content of 22 at.% the crystal size of TiC_xN_y is about 12 nm. The highest hardness of 41 GPa can be achieved for a silicon content of 12 at.%. A further increase of the silicon content leads to a remarkable decrease of the hardness. The TiSiCN coatings show a high oxidation resistance up to 900°C in dependence on the silicon content. The higher the silicon content the better the oxidation resistance. First wear tests by dry milling and dry boring of cast iron GGG40 show a higher tool life of the new TiSiCN coating in comparison to state-of-the-art PVD TiAlN layers. Due to high hardness and oxidation resistance as well as excellent wear behavior in machining cast iron CVD TiSiCN nanocomposite coating is a promising candidate for the next generation of wear resistant tool coatings.

Acknowledgements

The authors would like to thank Mr. Kolaska and the “Arbeitskreis Hartmetall” for the promotion of this work and Dr. Baumann of the company MAPAL for the conduction of the cutting tests.

References

[1] R.F. Bunshah, Handbook of Hard Coatings, Noyes Publications/William Andrew Publishing, LLC, Norwich, New York, U.S.A., 2001, page 377
[2] M. Wittmer, J. Noser. H. Melchior, Journal of Applied Physics 52 (1981) 6659
[3] J.H. Hsieh, A.L.K. Tan, X.T. Zeng, Surface & Coatings Technology 201 (2006) 4094
[4] T. Özel, T. Altan, International Journal of Machine Tools & Manufacture 40 (2000) 713
[5] S. Veprek, J. Vacuum Science and Technology A 17 (1999) 2401
[6] L. Shizhi, S. Yulong, P. Hongrui, Plasma Chemistry & Plasma Processing 12 (1992) 287
[7] I. Endler, E. Wolf, A. Leonhardt, V. Richter, Surface & Coatings Technology 72 (1995) 37
[8] S. Veprek, M. G. J. Veprek-Heijman, P. Karvankova, J. Prochazka, Thin Solid Films 476 (2005) 1
[9] C. T. Guo, D. Lee, P.C. Chen, Applied Surface Science 254 (2008) 3130
[10] Y. H. Cheng, T. Browne, B. Heckerman, E. I. Meletis, Surface & Coatings Technology 204 (2010) 2123
[11] J.-H. Jeon, S.R. Choi, W.S. Chung, K.H. Kim, Surface & Coatings Technology 188-189 (2004) 415
[12] R. Wei, C. Rincon, E. Langa, Journal of Vacuum Science and Technology A 28 (2010) 112
[13] D. Ma, S. Ma, H. Dong, K. Xu, T. Bell, Thin Solid Films 496 (2006) 438
[14] P. Jedrzejowski, J.E. Klemberg-Sapieha, L. Martinu, Thin Solid Films 466 (2004) 189
[15] S. Veprek, A. Niederhofer, K. Moto, T. Bolom, H.-D. Männling, P. Nesladek, G. Dollinger, A. Bergmaier, Surface & Coatings Technology 133-134 (2000) 152
[16] S. Veprek, M. Jilek, Vacuum 67 (2002) 443
[17] S.L. Ma, D.Y. Ma, Y. Guo, B. Xu, G.Z. Wu, K.W. Xu, P.K. Chu, Acta Materialia 55 (2007) 6350
[18] G. Llauro, R. Hillel, F. Sibieude, Chemical Vapor Deposition 4 (1998) 247
[19] K. Jun, Y. Shimogaki, Science and Technology of Advanced Materials 5 (2004) 549
[20] S. Hayashi, T. Hirai, K. Hiraga, M. Hirabayashi, Journal of Materials Science 17 (1982) 3336
[21] T. Hirai, S. Hayashi, Journal of Materials Science 18 (1983) 2401
[22] D.-H. Kuo, W.-C. Liao, Applied Surface Science 199 (2002) 278
[23] D.-H. Kuo, K.-W. Huang, Thin Solid Films 394 (2001) 81
[24] D.-H. Kuo, W.-C. Liao, Thin Solid Films 419 (2002) 11
[25] I. Endler, M. Höhn, J. Schmidt, S. Scholz, M. Herrmann, M. Knaut, Surface & Coatings Technology, 215 (2013), 133.
[26] R. Chatterjee-Fischer, P. Mayr, Proc. 5th European Conference on Chemical Vapour Deposition, June 17-20, 1985, Uppsala , Sweden, p. 395
[27] C. Czettl, C. Mitterer, U. Mühle, D. Rafaja, S. Puchner, H. Hutter, M. Penoy, C. Michotte, M. Kathrein, Surface & Coatings Technology 206 (2011) 1691
[28] A. Larsson, S. Ruppi, Thin Solid Films 402 (2002) 203
[29] C.T. Guo, D. Lee, P.C. Chen, Applied Surface Science 254 (2008) 3130
[30] G. Llauro, F. Gourbilleau, F. Sibieude, R. Hillel, Thin Solid Films 315 (1998) 336